Macromolecules

pubs.acs.org/Macromolecules Article

Investigation of Markovian and Non-Markovian Search Processes of Monomers of a Rouse Chain Confined in a Spherical Cavity

Ye Chen, Xiaofei Tian, Xiaolei Xu, Wen-Sheng Xu,* and Jizhong Chen*

Cite This: *Macromolecules* 2023, 56, 578−588

Read Online

ACCESS | Metrics & More | Article Recommendations

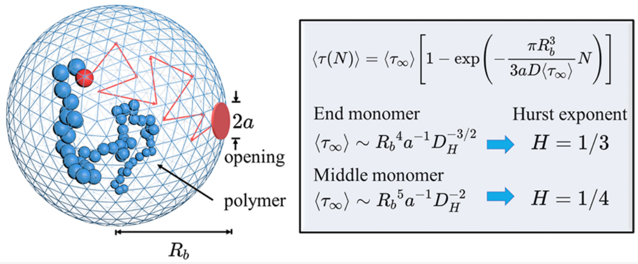

ABSTRACT: We study the process of monomers of a Rouse chain confined in a spherical cavity of radius R_b to search for a small opening of radius a on the cavity surface by combining scaling analysis and Langevin dynamics simulations. We show that the search process is nearly Markovian when the radius of gyration R_g of the chain is much smaller than R_b and becomes non-Markovian for $R_g \geq R_b$. For the non-Markovian search process, we first derive a general scaling relation for the mean search time $\langle\tau_\infty\rangle$ in the long chain limit and then explicitly determine the scaling exponents based on simulation results, $\langle\tau_\infty\rangle \sim R_b{}^4a^{-1}D_H{}^{-3/2}$ and $\langle\tau_\infty\rangle \sim R_b{}^5a^{-1}D_H{}^{-2}$ for the end and middle monomers, respectively, where D_H is a generalized diffusion coefficient associated with the monomer motion. We further find that the Hurst exponent, which characterizes the persistence of the dynamics, decreases exponentially from approximately 1/3 to about 1/4 as the monomer position changes from the end to the middle. This result implies that the subdiffusion of monomers depends considerably on their positions in the chain under confinement, providing insight into the anomalous dynamics of confined polymeric systems.

1. INTRODUCTION

The polymer escape problem has received extensive attention due to its importance in a number of physicochemical processes, including DNA packed inside virus capsids,[1−3] mRNA translocation from the nucleus via passive diffusion,[4,5] genome mapping,[6−8] polymer separation,[9,10] nucleotide sequencing,[11−15] etc. The quantity of main interest in this problem is the characteristic time for the movement of a chain from a confined space to an unconfined or larger space through a small opening. In general, polymer escape consists of two processes, namely, search and translocation.[16] The specific monomers of a polymer initially attempt to find the opening of the confined space, and after this search process is successful, the translocation starts. If the translocation process cannot be completed, additional search is then required. Notably, the search problem is also of high relevance to DNA repairing[17−21] and polymer binding[22,23] in a confined environment, where the polymer does not escape out of the bounded domain so that the search for monomers to find a given small target on the domain boundary is the key. Over the past decades, a number of theoretical and numerical studies have been focused on the translocation process,[24−29] where a significant progress has been achieved about the effects of various factors on the translocation process, such as the charge, driving force, and interactions between the chains and the pore. By contrast, much less is known about the physics underlying the search process.

In the present work, we focus on the search process of monomers of a Rouse chain under the confinement of a spherical cavity, as illustrated in Figure 1a, where we show a cartoon of a polymer chain confined in a spherical cavity of radius R_b having a small opening of radius a. As the simplest stochastic model of polymer dynamics, the Rouse model has been shown to be useful in explaining many aspects of polymer dynamics.[30] Unlike the translocation process where entropic barriers typically play a key role,[31−35] no significant changes in polymer conformations occur during the search process for openings without any barriers so that the search time is determined by the diffusion of monomers in various geometries. The calculation of this characteristic time is also known as the mean first passage time problem in stochastic theory.[36] In real systems, however, the openings are inevitably imperfect, so a diffusive particle often needs to overcome an energy or entropy barrier at the entrance to the opening to complete the search. Grebenkov and Oshanin[37] have shown that the narrow escape problem can be barrier-limited rather than diffusion-limited in the limit $a \to 0$.

Received: September 9, 2022
Revised: November 17, 2022
Published: January 10, 2023

https://doi.org/10.1021/acs.macromol.2c01877
Macromolecules 2023, 56, 578−588

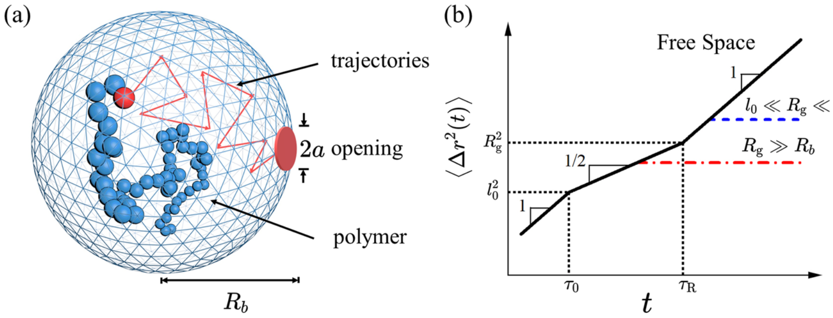

Figure 1. (a) Schematic illustration of a polymer chain confined in a spherical cavity of radius R_b having a small opening of radius a. To highlight the problem studied in the present work, one end of the polymer is shown by the red color, and the connected lines in red indicate the search process for the end monomer to find the opening by diffusion. (b) Illustration of the different regimes in the mean-square displacement $\langle \Delta r^2(t) \rangle$ of the monomer of a Rouse chain as a function of time t in free space and under confinement, as shown as the solid line and dashed and dash-dotted lines, respectively. Here, l_0 is the effective bond length, R_g is the radius of gyration, τ_0 is the typical relaxation time of a bond, and τ_R is the Rouse relaxation time.

To understand the diffusion of the monomer in the search process, let us first discuss the diffusion of monomers in free space. This topic is well documented in textbooks (e.g., ref 38), but we provide a recap to facilitate our discussion of monomer diffusion under confinement. For the monomers of a Rouse chain (Figure 1b), it is well established that three different regimes can be identified in the time (t) dependence of the mean-square displacement (MSD) $\langle \Delta r^2(t) \rangle$, as described by the following equation[38]

$$\langle \Delta r^2(t) \rangle = \begin{cases} 2dDt, & t < \tau_0 \\ Al_0{}^2(t/\tau_0)^{1/2}, & \tau_0 \le t < \tau_R \\ 2dD_{CM}t, & t \ge \tau_R \end{cases} \tag{1}$$

where the brackets $\langle ... \rangle$ denote the equilibrium ensemble averaging, d is the spatial dimension, D is the diffusion coefficient of the monomer, τ_0 is the typical relaxation time of a bond, A is a numerical coefficient, l_0 is the effective bond length, τ_R is the Rouse relaxation time, and D_{CM} is the diffusion of the center of mass of the chain. Note that D and D_{CM} are related simply via $D_{CM} = D/N$, where N is the number of the monomers in the polymer. First, in the short time limit, where $t < \tau_0$, the monomer is not affected by the connection with other monomers and moves as a Brownian particle with the diffusion coefficient D. When the time scale is longer than τ_0 but shorter than τ_R, the monomer motion is subdiffusive so that the MSD increases with time as $\langle \Delta r^2(t) \rangle \sim t^{1/2}$. Finally, the whole chain moves coherently so that all monomers essentially have the same diffusion coefficient as the chain (i.e., D_{CM}) at $t > \tau_R$. With this background, we next consider the diffusion of monomers of a Rouse chain confined in a cavity.

In a spherical cavity, it is evident that the diffusion of monomers depends on the extent of confinement, as characterized by the ratio of R_g to R_b, where R_g is the radius of gyration of the polymer in the absence of confinement. If R_g is much smaller than R_b, $\langle \Delta r^2(t) \rangle$ exhibits a plateau larger than $R_b{}^2$ at long t.[39] In such a case, the search process is dominated by the diffusion of the whole chain so that the subdiffusive motion of individual monomers becomes insignificant, and hence, the search follows a Markovian process. When R_g is comparable to or larger than R_b, the time at which $\langle \Delta r^2(t) \rangle$ starts to plateau lies in the regime $\tau_0 < t < \tau_R$.[40] This implies that the chain mobility is hindered by the confinement so that the anomalous diffusion of monomers is directly relevant to the search process.[41,42] Under such conditions, the search becomes a non-Markovian process, where the other monomers of the chain play the role of hidden degrees of freedom in affecting the motion of the tagged monomer.[43,44] Importantly, the non-Markovian phenomenon is fairly common in the context of other important problems of polymeric systems, including polymer looping,[45−47] binding,[48] and folding.[49]

We now discuss the estimation of the mean search time $\langle \tau \rangle$ for the monomers of a Rouse chain confined in a cavity for both the Markovian and non-Markovian processes. When the search follows a Markovian process, a Rouse chain can intuitively be viewed as a phantom Brownian particle, and the calculation of $\langle \tau \rangle$ is similar to that in the narrow escape problem of Brownian particles; hence, the problem is relatively straightforward to solve.[36] While it remains a challenge to predict $\langle \tau \rangle$ by stochastic theory for non-Markovian processes where the monomer exhibits subdiffusive behavior, previous computational works have yielded insights into the non-Markovian search process.[50−53] In particular, $\langle \tau \rangle$ has been found to depend on several physical factors,[50−53] such as the chain length and the sizes of the cavity and opening, as discussed below.

Holcman and co-workers[51] have shown based on Brownian dynamics (BD) simulations that $\langle \tau \rangle$ increases drastically with increasing N and eventually arrives at a plateau for sufficiently large N for a chain confined in a spherical cavity. Interestingly, this study also reveals that $\langle \tau \rangle$ depends on the monomer position in the chain. Moreover, Kantor and Kardar[52] have demonstrated that the probability density function of the search time for the middle monomer of a polymer still displays an exponential decay, although the confinement strongly affects the search process. Regarding the influence of the cavity size on $\langle \tau \rangle$, it is natural to expect that a longer time is required for a particle or monomer to find the opening as the cavity becomes bigger. Indeed, Grigoriev et al.[54] have shown that $\langle \tau \rangle \sim R_b{}^3$ for a Brownian particle in a spherical cavity. We must also mention the work of Voituriez and co-workers,[53] who have studied the search process of subdiffusive particles in a confined domain based on fractional BD simulations in $d = 2$, and their work indicates that $\langle \tau \rangle$ is related to the domain size R_b as $\langle \tau \rangle \sim R_b{}^{1/H}$, where H is the Hurst exponent characterizing the persistence of dynamics and is equal to 1/2 for a Brownian particle. Here, the persistence of dynamics is related to the long-range correlation between the displacements of the particle as a function of t. In the superdiffusive

https://doi.org/10.1021/acs.macromol.2c01877

regime with $1/2 < H < 1$, the dynamics is persistent so that positive correlations emerge, whereas in the subdiffusive regime with $0 < H < 1/2$, the dynamics becomes antipersistent so that negative correlations are expected.[55] Importantly, the analysis of Voituriez and co-workers[53] implies that dynamic persistence offers the potential to describe non-Markovian search processes, although whether or not dynamic persistence is relevant to the search process of polymers remains to be investigated. On the other hand, increasing the size of an opening or increasing the temperature of the system and thus the diffusion coefficient is expected to reduce $\langle\tau\rangle$. When a is much smaller than R_b, which is a common case in practice, it has been found that $\langle\tau\rangle$ of Brownian particles or monomers of a short chain is inversely proportional to a and D in a spherical cavity,[36,56] i.e., $\langle\tau\rangle \sim (aD)^{-1}$. Parenthetically, we note that the work of Singer et al.[57] indicates the relation $\langle \tau \rangle \sim R_b^{2}D^{-1} \ln(R_b/a)$ for a Brownian particle confined in a circular domain, demonstrating that the search process depends on spatial dimension, which can also be seen from the discussion of ref 53 above. Finally, we mention that knotted structures can significantly affect the translocation of polymers.[58]

It should be pointed out that the search process of a subdiffusive particle confined in a complex environment is ubiquitous in molecular and cellular biology,[59] although the treatment of such a problem is very difficult because of the boundary conditions associated with the geometrical structures.[60] In particular, because of complexities associated with the heterogeneity of porous structures and the underlying microscopic mechanisms, many problems remain to be explored in relation to transport in porous media. In this regard, single-particle tracking experiments[61,62] have provided a valuable method to directly investigate the influence of geometric parameters (e.g., pore size, pore throat size, and tracer particle size) and microscopic interaction parameters on the transport of particles and polymers in porous environments. Our point here is that the search process of a polymer confined in a cavity is truly a complicated problem. Even in the case of a Rouse chain confined in a spherical cavity, it remains unclear how the mean search time depends on the chain length, cavity size, opening size, and monomer diffusion when all these factors are taken into account. Here, we address this problem by combining scaling analysis and simulations.

In the present paper, we present a systematic study of the search processes of monomers of a Rouse chain confined in a spherical cavity. As expected, we find that the search process can be either Markovian or non-Markovian in a spherical cavity of fixed size, depending on the chain length. In the short chain limit, the search follows a Markovian process. In this relatively simple case, we show that simulation results for the mean search time $\langle\tau\rangle$ can be described quantitatively by a modified functional form derived from the search problem of a single Brownian particle confined in a spherical cavity.[51] In the long chain limit, the search process is dominated by the subdiffusive motion of monomers and thus becomes non-Markovian. On the basis of extensive simulation results, we identify a characteristic chain length N_c to describe the crossover from the Markovian to non-Markovian process. A detailed analysis of $\langle\tau\rangle$ for different monomers reveals that N_c is related to the number of monomers affected by the confinement in the chain. For the more complicated non-Markovian search process, we first derive a general scaling relation for the mean search time $\langle\tau_\infty\rangle$ in the long chain limit based on dimensional consistency and previous studies of the narrow escape problem of single particles.[54,56,57] We then utilize simulation results to explicitly determine the scaling exponents associated with the cavity size, opening size, and a generalized diffusion coefficient associated with the monomer motion for the end and middle monomers. We further discuss the search process of monomers other than the end and middle monomers based on simulation results. In particular, we examine the Hurst exponent H of different monomers to gain a better understanding of the non-Markovian search process. Our analysis indicates that H decreases exponentially from approximately 1/3 to about 1/4 as the monomer position changes from the end to the middle, implying that the subdiffusion of monomers depends considerably on their positions in the chain under confinement. Importantly, this crucial information cannot be obtained from the long-time plateau of the MSD. Our work thus provides insight into the anomalous dynamics of confined polymeric systems.

The remainder of the present paper is organized as follows. The simulation method is described in Section 2. Section 3 first provides a simple expression for the mean search time based on scaling analysis, followed by complementary simulation results to determine the unknown scaling exponents and a discussion of the Hurst exponent of different monomers in the chain. Finally, a summary is given in Section 4.

2. SIMULATION METHOD

The present work studies the search process of a linear Rouse chain confined in a spherical cavity, as shown in Figure 1a. In our model, the chain is composed of N monomers with the friction coefficient of $\xi = 1$, and adjacent monomers are connected by a spring stiffness of $k = 1$. Each monomer is viewed as a Brownian particle with the diffusion coefficient given by $D = k_BT/\xi$, where k_B is the Boltzmann constant and T is the temperature. Because the monomers in the Rouse model interact with each other only through the connected spring, the potential describing the model is given by

$$U_b = \frac{k}{2}\sum_{i=1}^{N}(\vec{x}_i - \vec{x}_{i-1})^2 \tag{2}$$

where x_i ($i = 1, ..., N$) is the coordinate of monomer i and $\vec{x}_0 = \vec{x}_1$ and $\vec{x}_{N+1} = \vec{x}_N$. For reference, the effective bond length is $l_0 = \sqrt{k_BT/k}$, the effective Kuhn length is $l_{\mathrm{Kuhn}} = \sqrt{3}\,l_0$, the radius of gyration is $R_g = l_0\sqrt{N/2}$, the bond relaxation time is $\tau_0 = \xi/k$, and the Rouse relaxation time is $\tau_R \approx R_g^{2}/D_{CM} = \tau_0N^2$.

To study the Rouse chain confined in a cavity, the repulsive, shifted and truncated Lennard-Jones repulsive potential with the energy scale of $\epsilon = 1$ is utilized to describe the interactions between monomers and the cavity boundary. More specifically, when a monomer approaches the cavity boundary, a repulsive interaction arises between the monomer and an imaginary bead of size l_0 on the cavity surface, as described by

$$U_{LJ}(r) = \begin{cases} 4\epsilon[(l_0/r)^{12} - (l_0/r)^{6}] + \epsilon, & r < r_{\mathrm{cut}} \\ 0, & r \geq r_{\mathrm{cut}} \end{cases} \tag{3}$$

where r is the distance between the monomer and the imaginary bead and the cutoff is $r_{\mathrm{cut}} = 2^{1/6}l_0$. In the present paper, length, time, and energy are reported in units of l_0, τ_0, and ϵ, respectively.

The equations of motion of a monomer are described by the overdamped Langevin equation

$$\xi \frac{d\vec{x}_i}{dt} = f_{1i} + f_{\text{wall}} + f_i^{\text{G}} \tag{4}$$

where $f_{1i} = -\nabla U_{\text{b}}$, $f_{\text{wall}} = -\nabla U_{\text{LJ}}$, and f_i^{G} is a Gaussian random noise having zero mean and satisfying the fluctuation–dissipation theorem, $\langle f_n^{\text{G}}(t) f_m^{\text{G}}(t')\rangle = 2\xi k_{\text{B}} T \delta_{n,m} \delta(t - t')$. The position of the monomer evolves at each time step via the following equation:

$$\vec{x}_i(t + \delta t) = \vec{x}_i(t) + \frac{1}{\xi}[f_{1i}(t) + f_{\text{wall}}(t)]\Delta t + \delta f_i^{\text{G}} \tag{5}$$

A time step of $\Delta t = 5 \times 10^{-4}\tau_0$ is used to integrate the equations of motion, which is sufficiently small to ensure the stability and accuracy of the simulations.[36]

In our simulations, the ratio a/R_{b} is varied from 0.05 to 0.2, following the work of Schuss.[60] Initially, all monomers are placed close to the center of the cavity and are folded on the top of each other. The data are collected after the system has been equilibrated for a period much longer than τ_{R}, and proper equilibration is confirmed by utilizing different initial chain conformations and extending the run time by a factor of 3 or larger. Each run is terminated after the tagged monomer finds the opening for the first time. The results in the present paper are obtained by performing the average over at least 4000 runs.

3. RESULTS AND DISCUSSION

This section begins with a scaling analysis of the mean search time, followed by detailed simulation results to determine the unknown exponents in the scaling relation. This section then utilizes the Hurst exponent to gain a better understanding of the non-Markovian search process of different monomers in the chain, inspired by the work of Voituriez and co-workers.[53]

3.1. Scaling Analysis of Mean Search Time.

We provide a scaling analysis of the mean search time $\langle\tau\rangle$ of monomers of a Rouse chain confined in a spherical cavity of radius R_{b} having a small opening of radius a. In particular, we consider the dependence of $\langle\tau\rangle$ on the relevant variables, including R_{b}, a, and the monomer diffusion. Let us first focus on the relatively simple case where the chain size is much smaller than the cavity size. In such a case, since the search process is dominated by the chain diffusion, it is reasonable to treat the chain as a phantom Brownian particle having a radius of R_{g} and a diffusion coefficient of D_{CM}. When the opening area is much less than the surface area of the cavity, which is usually the case in practice, the mean search time $\langle\tau\rangle$ can be described by[56,57,60,63]

$$\langle\tau\rangle \approx \frac{V}{4aD_{\text{CM}}} = \frac{\pi N R_{\text{b}}^3}{3aD} \tag{6}$$

where $V = 4\pi R_{\text{b}}^3/3$ is the volume of the spherical cavity. However, if the chain effects are not negligible, eq 6 should be modified as[51]

$$\langle\tau\rangle \approx \frac{\pi N (R_{\text{b}} - R)'^3}{3aD} \tag{7}$$

where the correction term R' depends on the position of the tagged monomer. Holcman and co-workers[51] have found that a reasonable estimate of R' for the end monomer is given by R_{g}.

Here, to put the magnitude of $\langle\tau\rangle$ in perspective, we can make a comparison between the mean search time and the longest relaxation time of the Rouse chain, τ_{R}, which is the characteristic time for the chain to move a distance of the order of its own size. It is evident that $\langle\tau\rangle > \tau_{\text{R}}$ in the case of $R_{\text{g}} \ll R_{\text{b}}$. On the other hand, if the search process is dominated by the subdiffusive motion of monomers, the mean search time is expected to be shorter than the Rouse relaxation time, i.e., $\langle\tau\rangle < \tau_{\text{R}}$.

We now turn to the more complicated case where the chain size is comparable to or larger than the cavity size. As illustrated in Figure 1b, the MSD of the monomers in a spherical cavity is diffusive at short t and then subdiffusive at intermediate t before reaching a plateau at long t. The search process typically depends on the diffusion behavior of monomers at long t. However, the long-t plateau cannot determine whether or not the long-t dynamics of the monomers follows the subdiffusive motion at intermediate t. To be sufficiently general, we thus write the t-dependent MSD of a monomer in the following form

$$\langle\Delta r^2(t)\rangle \sim D_H t^{2H} \tag{8}$$

where D_H is a generalized diffusion coefficient. Here, the cases of $1/2 < H < 1$, $H = 1/2$, and $0 < H < 1/2$ correspond to the superdiffusive motion of the monomer, the Brownian motion, and the subdiffusive motion, respectively. We expect $\langle\tau\rangle$ to depend only on D_H, H, a, and R_{b}. Analysis based on the dimensional consistency then implies the following form

$$\langle\tau\rangle \simeq \left(\frac{R_{\text{b}}^2}{D_H}\right)^{1/(2H)} f\left(\frac{a}{R_{\text{b}}}\right) \tag{9}$$

where f is a dimensionless function. In the case of a spherical cavity, previous studies on the narrow escape problem of single particles have indicated that $\langle\tau\rangle$ is related to R_{b} by the power law,[54,56,57] $\langle\tau\rangle \sim R_{\text{b}}^{\alpha}$, with α being a scaling exponent. The expression for $\langle\tau\rangle$ can then be written as

$$\langle\tau\rangle \sim R_{\text{b}}^{\alpha} a^{\beta} D_H^{\gamma} \tag{10}$$

where the scaling exponents α, β, and γ should satisfy the following relation

$$\alpha + \beta + 2\gamma = 0 \tag{11}$$

with $\gamma = -1/(2H)$. Evidently, a monomer is more difficult to search for the opening in a larger cavity, whereas a larger opening or a faster monomer motion should speed up the search process. Hence, α is expected to be positive, and both β and γ should be negative. Theoretical and numerical studies of simple Brownian particles have shown that $\alpha = 3$, $\beta = -1$, and $\gamma = -1$,[36,57,60] thereby satisfying eq 11. However, the estimates of the scaling exponents α, β, and γ have not yet been made for polymers. In the present work, we determine these scaling exponents with the aid of simulation results, as discussed below.

3.2. Chain Length Dependence of Mean Search Time and Simulation Estimates of the Scaling Exponents.

Our analysis based on simulation results starts with the dependence of $\langle\tau\rangle$ on N. In our simulations, the mean search time is determined from the survival probability $S(t)$ of the monomer in the cavity[54]

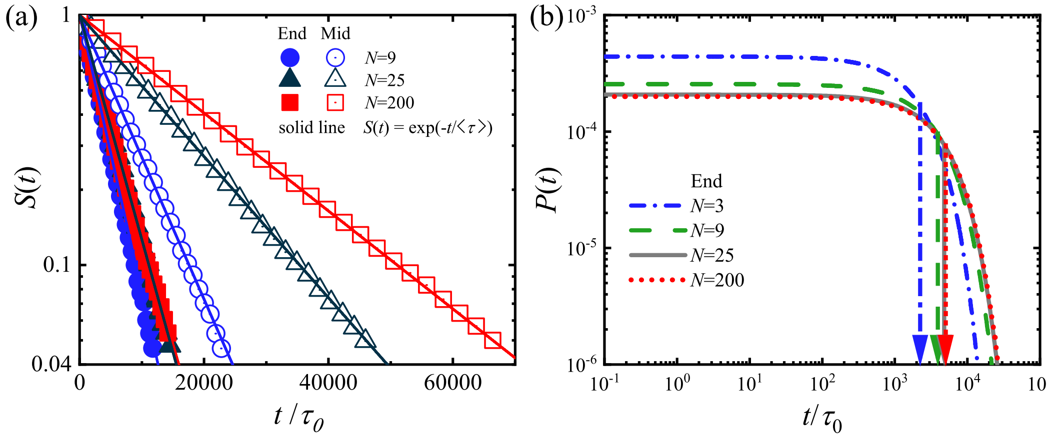

Figure 2. (a) Survival probability $S(t)$ of monomers of a Rouse chain confined in a spherical cavity of $R_\mathrm{b} = 10\ l_0$ and $a = l_0$ at $k_\mathrm{B}T/\epsilon = 1$ for different chain lengths N. Filled and opens symbols correspond to the results of the end and middle monomers, respectively. Solid lines represent the fits of an exponential function to the simulation data at long t. (b) Probability distribution function $P(t)$ of the search times of the end monomer of a Rouse chain confined in a cavity of $R_\mathrm{b} = 10\ l_0$ and $a = l_0$ at $k_\mathrm{B}T/\epsilon = 1$ for different N. Vertical arrows indicate the mean search times.

$$S(t) = \frac{1}{N_\mathrm{s}}\sum_{j=1}^{N_\mathrm{s}} H(\tau_j - t) \tag{12}$$

where N_s is the number of statistical samples, τ_j is the search time of the jth sample, and $H(t)$ is the Heaviside step function. $\langle\tau\rangle$ can then be obtained as $\langle\tau\rangle = (1/N_\mathrm{s})\sum_{j=1}^{N_\mathrm{s}}\tau_j$.

In general, the search for an opening is a long-time behavior. A previous study for the diffusion of a very long Rouse chain between two absorbing boundaries has shown that $S(t)$ for the middle monomer decays exponentially at long t.[52] Our simulation results of $S(t)$ are consistent with this behavior, as shown in Figure 2a, where we show $S(t)$ of the end and middle monomers of a Rouse chain confined in a spherical cavity of $R_\mathrm{b} = 10\ l_0$ and $a = l_0$ at $k_\mathrm{B}T/\epsilon = 1$ for different N. Hence, the mean search time can also be determined by the characteristic time describing the decay of the survival probability.[56]

$$S(t) = \exp(-t/\langle\tau\rangle) \tag{13}$$

In the present work, we show the results of $\langle\tau\rangle$ from the exponential fits. Notably, the translocation should start from one end of the chain in the context of polymer translocation. By contrast, the search process of monomers of a chain has implications for a broader range of problems. The search process is not only an important step for polymer translocation, but it is also relevant in other problems. For instance, when a specific segment of polymers (DNA or mRNA) searches for specific receptors to trigger reaction,[36] this segment can be the end, middle, or other monomers in the chain, which has been demonstrated explicitly in the literature.[51,52,64]

While the mean search time is evidently an important quantity for understanding the search process, a more complete picture can be provided by the full distribution of the search times. In this regard, Oshanin and co-workers[65] have recently made a progress in the case of diffusive particles by deriving the full first-reaction time (FRT) distribution for the narrow escape problem. This work indicates that typical FRTs may be orders of magnitude shorter than the mean one, leading to a strong defocusing of characteristic time scales. Motivated by ref 65, we also analyze the probability distribution function $P(t)$ of the search times, as determined by the derivative of the survival probability, i.e., $P(t) = -\mathrm{d}S(t)/\mathrm{d}t$. As an example, Figure 2b shows $P(t)$ of the end monomer of a Rouse chain confined in a cavity of $R_\mathrm{b} = 10l_0$ and $a = l_0$ at $k_\mathrm{B}T/\epsilon = 1$ for different N. For reference, the plot includes vertical arrows to indicate $\langle\tau\rangle$. As can be seen, $P(t)$ exhibits a plateau at short t that first decreases with increasing N and becomes independent of N for large N. At long t, an exponential tail is evident for $P(t)$, indicating that $\langle\tau\rangle$ corresponds to the characteristic time of the exponential decay. Hence, the features of $P(t)$ for the Rouse chain are qualitatively similar to those of diffusive particles considered by Oshanin and co-workers.[65] Evidently, $P(t)$ should make an attractive target for future study. In the present work, however, we focus on $\langle\tau\rangle$ as our first step toward a deep understanding of the search process of polymers confined in a cavity.

Figure 3 shows $\langle\tau\rangle$ as a function of N determined from our simulations for the end and middle monomers of a Rouse chain confined in a spherical cavity of $R_\mathrm{b} = 10l_0$ and $a = l_0$ at $k_\mathrm{B}T/\ \epsilon = 1$. As can be seen, $\langle\tau\rangle$ for both the end and middle monomers increase with increasing N and plateau at

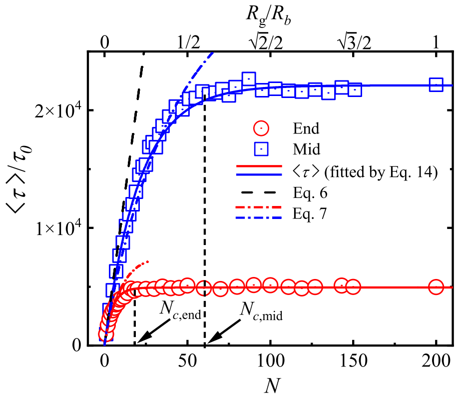

Figure 3. Mean search time $\langle\tau\rangle$ as a function of N for the end and middle monomers of a Rouse chain confined in a spherical cavity of $R_\mathrm{b} = 10l_0$ and $a = l_0$ at $k_\mathrm{B}T/\epsilon = 1$. Solid lines represent the fits of eq 14 to the simulation data. The long dashed line corresponds to eq 6. The dash-dotted lines correspond to eq 7 with $R' = R_\mathrm{g}$ and $R_\mathrm{g}/2$ for the end and middle monomers, respectively. For reference, the ratio $R_\mathrm{g}/R_\mathrm{b}$ is shown on the top axis.

sufficiently large N. We find that the simulation data can be well described by

$$\langle \tau(N)\rangle = \langle \tau_\infty\rangle\left[1 - \exp\left(-\frac{\langle \tau_s\rangle}{\langle \tau_\infty\rangle}N\right)\right] \tag{14}$$

where $\langle \tau_\infty\rangle$ is the long chain limit of $\langle \tau(N)\rangle$ and $\langle \tau_s\rangle \approx \pi R_b^3/(3aD)$ is the mean search time of a single monomer. The fitted results are shown as solid lines in Figure 3. In the limit of $N \to 1$, where the chain effects vanish, eq 14 reduces to eq 6 (see the long dashed line in Figure 3). In this case, the chain behaves as a phantom Brownian particle of R_g with the diffusion coefficient given by $D_{CM} = D/N$, and the end and middle monomers have the same mean search time that increases linearly with N. As N increases, the chain effects set in and the monomer position in the phantom particle must be considered.

As shown in Figure 4, the probability distribution functions $P(r)$ for the end and middle monomers relative to the center of mass of an unconfined Rouse chain display peaks at R_g and $R_g/2$, respectively. Substituting $R' = R_g$ for the end monomer and $R' = R_g/2$ for the middle monomer into eq 7 leads to good agreement with the simulation data for short chains, as shown by the dash-dotted lines in Figure 3. The insets of Figure 4 show cartoons of the difference between the search processes of the end and middle monomers. For the end monomer, finding the opening corresponds to the situation when the surface of the phantom particle encounters the opening. In contrast, the phantom particle must travel an extra distance of $R_g/2$ for the middle monomer to approach the opening. In this sense, the end monomer is more easily affected by the confinement than the middle monomer. This leads to the difference in the characteristic chain lengths where $\langle \tau\rangle$ starts to be independent of N, as shown Figure 3. In particular, Figure 5 shows the power-law dependences of the characteristic chain length on R_b, i.e., $N_{c,\mathrm{end}} \sim R_b$ for the end monomer and $N_{c,\mathrm{mid}} \sim R_b^2$ for the middle monomer, respectively. Below, we define $N_{c,\mathrm{mid}}$ as the characteristic chain length N_c for a Rouse chain confined in a given cavity, for which the mean search times of all monomers in the chain are independent of N.

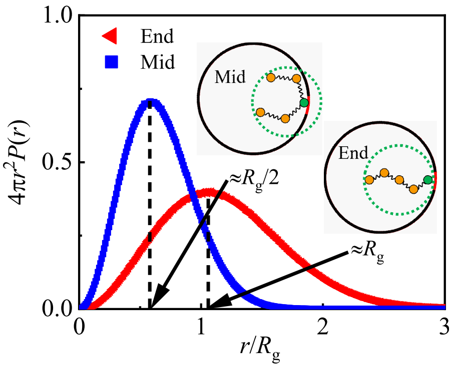

Figure 4. Probability distribution functions $P(r)$ of the end and middle monomers relative to the center of mass of a Rouse chain with $N = 8$ at $k_BT/\epsilon = 1$ in the absence of confinement. The insets depict the difference between the search processes of the end and middle monomers.

On the basis of the above results, we can provide reasonable estimates of the scaling exponents associated with the expressions of $\langle \tau_\infty\rangle$ for the end and middle monomers. For a confined Rouse chain, we expect that $N_{c,\mathrm{end}}$ depends only on R_b and l_0, namely, $N_{c,\mathrm{end}} \sim R_b/l_0 = R_b\sqrt{k/k_BT}$. It follows from eq 14 that $N_{c,\mathrm{end}} \sim \langle \tau_\infty\rangle/\langle \tau_s\rangle \approx 3aD\langle \tau_\infty\rangle/\pi R_b^3 = 3ak_BT\langle \tau_\infty\rangle/\xi\pi R_b^3$ for the end monomer. Combining eq 10 and the relation $D_H \sim k_BT$, we then obtain $\alpha = 4$, $\beta = -1$, and $\gamma = -3/2$ for the end monomer. In a similar manner, $\alpha = 5$, $\beta = -1$, and $\gamma = -2$ are obtained for the middle monomer. Therefore, we can arrive at the following scaling relations

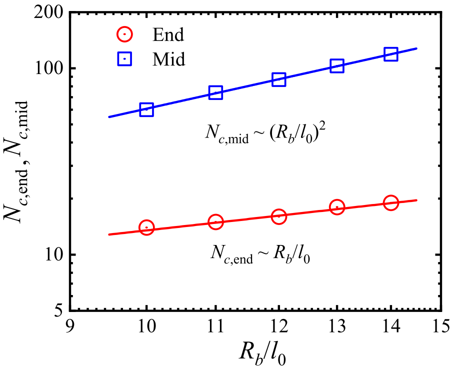

Figure 5. Characteristic chain lengths $N_{c,\mathrm{end}}$ and $N_{c,\mathrm{mid}}$ for the end and middle monomers as a function of R_b. The lines correspond to the power-law fits to the simulation data based on $N_{c,\mathrm{end}} \sim R_b$ and $N_{c,\mathrm{mid}} \sim R_b^2$ for the end and middle monomers, respectively.

$$\langle \tau_\infty\rangle \sim R_b^4 a^{-1} D_H^{-3/2} \text{ and } \langle \tau_\infty\rangle \sim R_b^5 a^{-1} D_H^{-2} \tag{15}$$

for the mean search times of the end and middle monomers in the long chain limit, respectively. In the following, we present detailed simulation results on the dependences of $\langle \tau_\infty\rangle$ on R_b, a, and D_H for $N \gg N_c$ to check the scaling relations of eq 15 and gain physical insights into these relations.

Before leaving the present section, it is worth examining the dependence of $\langle \tau_\infty\rangle$ on monomer position i in the chain. Taking the symmetry of a linear chain into account, it is adequate to consider the results of monomers with $i \le N/2$. As shown in Figure 6, $\langle \tau_\infty\rangle$ increases with i for $i < N_c/2$ and is essentially independent of i for $i > N_c/2$. If a tagged monomer can be regarded as being connected to two chains of different length, the dependence of $\langle \tau_\infty\rangle$ on the monomer position

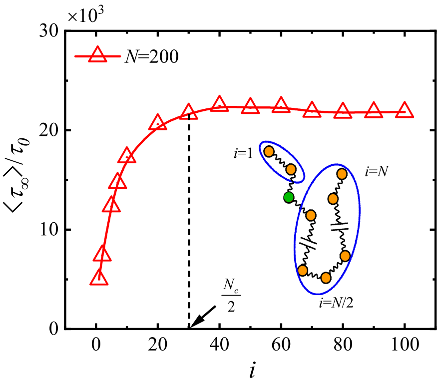

Figure 6. Dependence of $\langle \tau_\infty\rangle$ on the monomer index i for a Rouse chain with $N = 200$ confined in a spherical cavity of $R_b = 10l_0$ and $a = l_0$ at $k_BT/\epsilon = 1$. The inset shows the cartoon of a Rouse chain with the monomer index ranging from 1 to N. A tagged monomer, shown in green, can be regarded as being connected to two chains of different length.

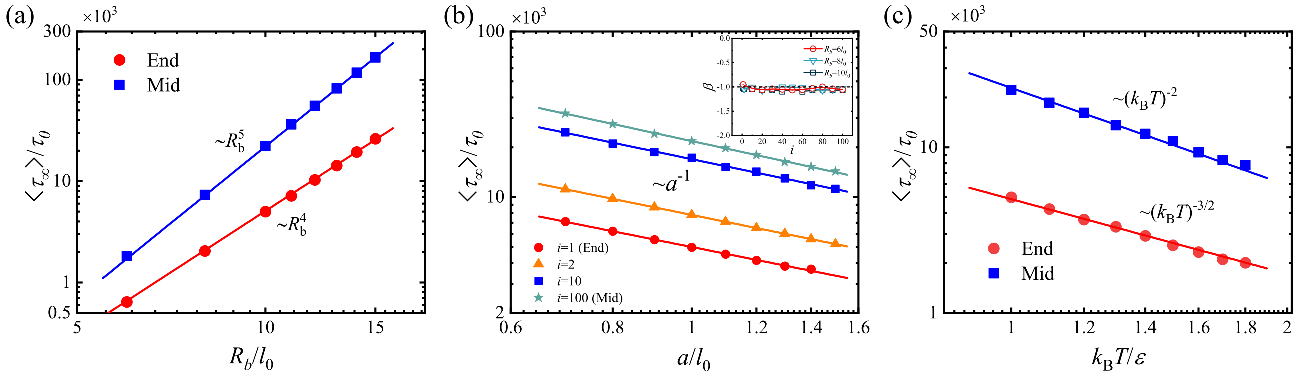

Figure 7. (a) $\langle\tau_\infty\rangle$ of the end and middle monomers as a function of R_b for a Rouse chain with $N = 200$ confined in a spherical cavity of $a = l_0$ at $k_BT/\epsilon = 1$. Solid lines correspond to the power-law fits, $\langle\tau_\infty\rangle \sim R_b^\alpha$, where α are determined to be 4 and 5 for the end and middle monomers, respectively. (b) $\langle\tau_\infty\rangle$ as a function of a for different monomer positions i for a Rouse chain with $N = 200$ confined in a spherical cavity of $R_b = 10l_0$ at $k_BT/\epsilon = 1$. Solid lines correspond to the power-law fits, $\langle\tau_\infty\rangle \sim a^\beta$, where the determined β is shown as a function of i for different R_b in the inset. (c) $\langle\tau_\infty\rangle$ of the end and middle monomers as a function of k_BT/ϵ for a Rouse chain with $N = 200$ confined in a spherical cavity of $R_b = 10l_0$ and $a = l_0$. Solid lines correspond to the power-law fits, $\langle\tau_\infty\rangle \sim T^\gamma$, where γ are determined to be $-3/2$ and -2 for the end and middle monomers, respectively.

arises from the effects of the shorter chain, as illustrated in the inset of Figure 6. In this sense, N_c characterizes the number of monomers affected by the confinement in the chain.

3.3. Dependence of Mean Search Time on Cavity Size, Opening Size, and Temperature.

Here, we perform a range of simulations to examine the dependence of the mean search time on the cavity size, opening size, and diffusion coefficient, which allows us to estimate the scaling exponents independently. We first focus on the scaling exponent α in eq 10 for the end and middle monomers. In this set of simulations, the cavity radius is varied from $R_b = 6l_0$ to $14l_0$, while the opening size is fixed at $a = l_0$ to ensure that the opening area is much less than the surface area of the cavity in each case, the chain length is fixed at $N = 200$, and D_H is kept at constant by $k_BT/\epsilon = 1$. Figure 7a shows $\langle\tau_\infty\rangle$ of the end and middle monomers as a function of R_b. In the range of R_b considered, N_c for the middle monomer varies from 22 to 118, which are smaller than the chain length considered. In line with our scaling analysis in Section 3.1, the simulation data can be described by a power law, $\langle\tau_\infty\rangle \sim R_b^\alpha$, where the exponents α are determined to be 4 and 5 for the end and middle monomers, respectively. These values are thus in good agreement with our analysis of eq 15 in Section 3.2.

For monomers other than the end and middle monomers, unfortunately, the above method fails to provide an estimate of α. When varying the cavity size in the long chain limit, the middle monomer is tethered by two chains with lengths larger than $N_c/2$ so that the end monomer has no effect on the search process of the middle monomer. In contrast, the end monomer drags a chain with the length of $N_c/2$ to search for the opening. As shown above, N_c increases with increasing R_b. Because polymers possess fractal properties, only the relative location of the end monomer in the dragged chain remains constant in the current dispersed chain model, but the relative locations of other monomers affected by the end are varied by changing R_b. This leads to the dependence of α on R_b and thus N_c for monomers with $1 < i \leq N_c$, for which the search dynamics is influenced by the end monomer. In other words, α is not constant for these monomers. We will further discuss this issue below.

Regarding the scaling exponent β, Figure 7b shows $\langle\tau_\infty\rangle$ as a function of a for different monomer positions i for a Rouse chain with $N = 200$ confined in a spherical cavity of $R_b = 10l_0$ at $k_BT/\epsilon = 1$. Here, a is varied from $0.7l_0$ to $1.5l_0$, which ensures that the ratio of the opening area to the surface area of the cavity is small. As can be seen, simulation data for all monomers can be well fitted by a power law, $\langle\tau_\infty\rangle \sim a^\beta$, where we determine $\beta = -1$ with a relative error less than 0.06, thereby confirming our analysis of eq 15 in Section 3.2. Notably, the same value is also found for β in the case of a Brownian particle.[56] The inset of Figure 7b shows that β for the monomers of the chain with $N = 200$ confined in cavities having different R_b are all close to -1, indicating that β is independent of the monomer position in the chain for sufficiently large N, in contrast to the scaling exponent α.

Finally, it is difficult to determine the scaling exponent γ by directly examining $\langle\tau_\infty\rangle$ as a function D_H because D_H is not an input parameter in a simulation. Fortunately, because D_H is proportional to T in our model, γ can be alternatively estimated by studying the dependence of T on $\langle\tau_\infty\rangle$. Figure 7c shows $\langle\tau_\infty\rangle$ of the end and middle monomers of a Rouse chain with $N = 200$ confined in a cavity of $R_b = 10l_0$ as a function of T. As expected, $\langle\tau_\infty\rangle$ decreases with increasing T via a power law, $\langle\tau_\infty\rangle \sim T^\gamma$, where γ are determined to be $-3/2$ and -2 for the end and middle monomers, respectively. These scaling exponents are again fully consistent with those obtained in Section 3.2.

As in the estimate of α, the scaling exponent γ for other monomers influenced by the end monomer (i.e., $1 < i \leq N_c/2$) cannot be determined based on the above method because the chain size depends on T. In particular, when T is varied, the characteristic chain length in a given cavity changes simultaneously, thereby leading to the dependence of γ on T for these monomers. Nevertheless, our simulation results in this section verify our analysis of the end and middle monomers based on the scaling approach in Sections 3.1 and 3.2.

3.4. Understanding Non-Markovian Search Process Based on the Hurst Exponent.

We now examine the Hurst exponent H to gain a better understanding of the non-Markovian search process of different monomers in the chain. It follows from $H = -1/(2\gamma)$ that H are 1/3 and 1/4 for the end and middle monomers in the long chain limit, $N > N_c$. For the end monomer, the Hurst exponent deviates from the

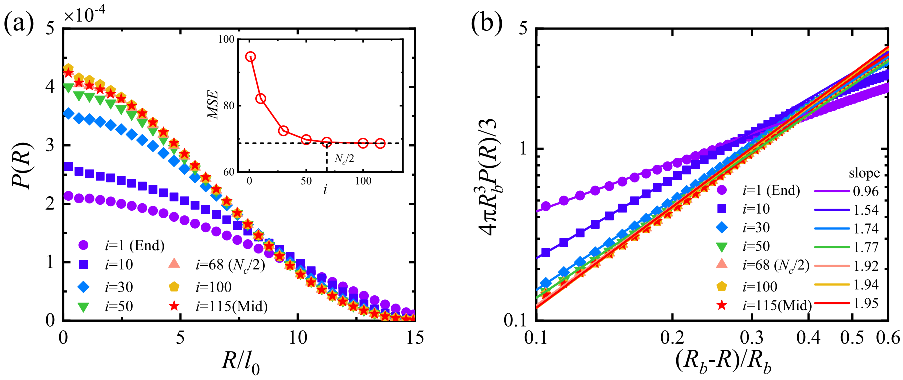

Figure 8. (a) Probability distribution function $P(R)$ of different monomers in the Rouse chain with $N = 230$ in a closed spherical cavity of $R_b = 15l_0$ at $k_BT/\epsilon = 1$. The inset shows the mean square error (MSE) of $P(R)$ as a function of the monomer index i. (b) Power-law dependence of the scaled probability density $4\pi R_b^3P(R)/3$ on the scaled distance $(R_b - R)/R_b$ from the wall for different monomer positions i. As indicated by the legend, the power-law exponent decreases from values near −1 to values close to −2 as i increases and starts to plateau approximately at $i = N_c/2$.

subdiffusive motion of the Rouse model in free space, which cannot directly be measured due to this anomalous dynamical behavior in the long-time plateau of the MSD. From a physics point of view, a smaller H indicates that the particle has a stronger antipersistence. If the distribution of a subdiffusive particle within a confined space is inhomogeneous, the particle tends to return to the center of the confined space.[55] This phenomenon is also seen in the search process of monomers of a Rouse chain confined in a cavity.[50,51]

Figure 8a shows the probability distribution function $P(R)$ of different monomers in the Rouse chain with $N = 230$ in a cavity of $R_b = 15l_0$, where R is the distance between a monomer and the center of the cavity. We see that the distribution of each monomer is nonuniform. Moreover, $P(R)$ is insensitive to changes in i when i is sufficiently large. The inset of Figure 8a shows the mean square error (denoted by MSE) of $P(R)$, which is defined by MSE $= \int_0^{R_b} R^2P(R)4\pi R^2\, dR$.[66] As can be seen, this quantity decreases as the monomer index increases and eventually arrives at a plateau approximately at $i = N_c/2$. This result indicates that the monomers with $N_c/2 \le i \le N/2$ have the same $P(R)$.

Vojta et al.[55] have proposed that the distribution of a particle in a cavity can be related to the Hurst exponent H via the following empirical equation

$$P(R) \sim \left(1 - \frac{R}{R_b}\right)^{1/H-2} \tag{16}$$

We find that the above relation works well in the range of R close to the cavity boundary and provides a good description of the distribution of monomers in the range $0.4R_b \lesssim R \lesssim 0.9R_b$, as shown in Figure 8b. Hence, this analysis allows us to obtain an estimation of H for each monomer.

Figure 9 shows H for different monomers of the Rouse chains with $N = 230$ and 500 confined in cavities of $R_b = 15l_0$ and $25l_0$, respectively, for which the corresponding characteristic chain lengths are $N_c = 136$ and 366. This analysis shows that H is nearly equal to 1/3 for the end monomer and independent of R_b, consistent with the analysis of $\langle\tau_\infty\rangle$. Similarly, we find $H \approx 1/4$ for monomers $N_c/2 \le i \le N/2$ in both cases considered. Remarkably, H exhibits a significant dependence on R_b for monomers $1 < i < N_c/2$, implying that $\langle\tau_\infty\rangle$ for these monomers do not obey the power-law dependence on R_b and D_H so that eq 10 fails to describe $\langle\tau_\infty\rangle$ of these monomers. Therefore, the above analysis demonstrates the importance of H in understanding the anomalous dynamics of confined polymeric systems.

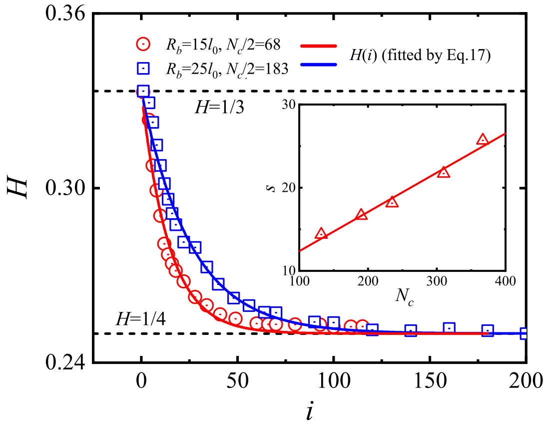

Figure 9. Hurst exponent H as a function of the monomer index i for the Rouse chains with $N = 230$ and 500 confined in cavities of $R_b = 15l_0$ and $25l_0$ at $k_BT/\epsilon = 1$, respectively. Solid lines correspond to the fits of eq 17. The inset shows the fitted parameter s as a function of N_c.

As a final remark, the solid lines in Figure 9 indicate that the dependence of H on the monomer position i can be described by

$$H(i) = H(N/2) + [H(1) - H(N/2)]\exp(-si) \tag{17}$$

where s is a fitting parameter. The inset of Figure 9 indicates that s is proportional to N_c to a good approximation. We note that eq 17 is more accurate for larger R_b (and thus N_c). This is attributed to the fact that increasing the ratio of R_b to l_0 may significantly reduce numerical errors in the current dispersed chain model. Unfortunately, an increase in R_b leads to a dramatic increase in simulation time; e.g., our result indicates $\langle\tau_\infty\rangle \sim R_b^5$ for the middle monomer. Hence, it becomes very difficult to examine the validity of eq 17 in the limit of $R_b/l_0 \to \infty$ using simulations.

4. SUMMARY

We have investigated the search processes of monomers of a Rouse chain confined in a spherical cavity. The extent of confinement has crucial effects on the search process. Accordingly, the search process can be classified into two types: Markovian and non-Markovian. When the chain size is much smaller than the cavity size, the monomer moves essentially as a phantom Brownian particle and the search follows a Markovian process. However, when the chain size is comparable to or larger than the cavity size, the subdiffusive motion of monomers dominates the search process so that a non-Markovian process emerges. This point can be rationalized based on the following considerations. Imagine that the cavity opening is sufficiently small so that the polymer can reasonably viewed as being confined in a closed spherical cavity. In that case, the search time of the monomer tends to be infinite. Take the end monomer as an example, if the search process of the long chain is dominated by the normal diffusion, the position distribution of the end monomer in the closed cavity should be uniform over a long period of time. This can be checked directly based on simulations. We found that the end monomers are uniformly distributed in the cavity in the case of short chains, but the end monomers for long chains tend to be near the center of the cavity (data not shown). Hence, the search process of the end monomer of long chains should be dominated by subdiffusion rather than normal diffusion. Moreover, the search time of the monomer is found to be smaller than the chain relaxation time, which is another evidence that subdiffusion should dominate the search process.

The search process can be quantitatively characterized by the mean search time $\langle\tau\rangle$. We have shown that the dependence of $\langle\tau\rangle$ for the end and middle monomers on the chain length N in a given cavity can be described by an exponential function linking the mean search time of a single particle, $\langle\tau_s\rangle$, to that in the long chain limit, $\langle\tau_\infty\rangle$. In the short chain limit, a reasonable estimate of $\langle\tau\rangle$ for both the end and middle monomers can be provided by a modified functional form derived from the search problem of a Brownian particle according to their positions relative to the center of mass of the particle. We have identified a characteristic chain length N_c to characterize the crossover from the Markovian to the non-Markovian process. Our analysis has indicated that N_c is related to the number of monomers affected by the confinement in the chain. For the more complicated non-Markovian search process, we have derived a general scaling relation for $\langle\tau_\infty\rangle$ based on dimensional consistency and previous studies of the narrow escape problem of single particles.[54,56,57] We have utilized simulation results to explicitly determine the scaling exponents associated with the cavity size, opening size, and a generalized diffusion coefficient associated with the monomer motion for the end and middle monomers.

Importantly, we have examined the Hurst exponent H of different monomers to gain a better understanding of the non-Markovian search process. In particular, H has been shown to be 1/3 and 1/4 for the end and middle monomers in the long chain limit, and hence, the long-time dynamics are different for these monomers. For the end monomer, the deviation from the well-known subdiffusive motion of the Rouse model implies anomalous dynamics of a confined Rouse chain, and this dynamical behavior cannot be resolved from the long-time plateau of the mean square displacement. To confirm this finding, we have calculated H for different monomers by analyzing the distribution of monomers in the cavity as suggested by Vojta et al.[55] This analysis has indicated that confinement has key effects on the dynamics of different monomers in the chain. The number of affected monomers turns out to be characterized by N_c, as noted above. We have also proposed an empirical formula for H as a function of the monomer position in the limit of $N > N_c$. Overall, our results are expected to be useful for understanding the anomalous dynamics of confined polymeric systems.

It should be mentioned that the present work has focused on the search process of monomers of a Rouse chain in a spherical cavity. In real systems such as cells, the confined domain is typically irregular. Studies on the mean first passage time problem of Brownian particles have revealed that the geometry of the confined domain can dramatically influence the search process, a problem that would be also of great relevance to polymeric systems. The present work also does not take into account surface interactions, which are a common feature in cells. Adding a surface interaction reduces the dimension in which diffusion occurs from the three-dimensional space to two-dimensional surface diffusion.[67] In this situation, the efficiency of particle search can be better than that of direct search in three-dimensional space under certain conditions.[68] However, this problem is expected to be more complicated for polymers than for particles. Moreover, the Rouse model neglects the excluded volume interactions between monomers, a factor that has been known to affect the monomer distributions of both free and confined polymers.[69] Hence, the effect of the excluded volume interactions on the search process also deserves a detailed study in future work. Notably, the quantity of central interest is the *attempt* time in ref 69. This characteristic time scale is important for understanding the translocation process of confined polymers but differs from the search time considered in the present work. Crowding is also one of the main characteristics of chain movement in living cells. Indeed, the role of crowding on polymer looping has been studied. Metzler and co-workers[70] have investigated the looping dynamics of flexible polymer chains in the presence of different degrees of crowding, revealing that small crowders typically slow down the chain dynamics, but the looping may be facilitated by larger crowders. Zhao and co-workers[71] have proposed a statistical model to understand the anomalous looping kinetics in polymer solutions, unambiguously highlighting the impact of polymer crowding on the loop formation rate. Therefore, crowding is expected to be also a potential factor in affecting the search dynamics of polymers confined in a cavity.

■ AUTHOR INFORMATION

Corresponding Authors

Wen-Sheng Xu − *State Key Laboratory of Polymer Physics and Chemistry, Changchun Institute of Applied Chemistry, Chinese Academy of Sciences, Changchun 130022, P. R. China; University of Science and Technology of China, Hefei 230026, P. R. China*; Email: wsxu@ciac.ac.cn

Jizhong Chen − *School of Chemical Engineering and Light Industry, Guangdong University of Technology, Guangzhou 510006, P. R. China*; Email: jzchen@gdut.edu.cn

Authors

Ye Chen − *State Key Laboratory of Polymer Physics and Chemistry, Changchun Institute of Applied Chemistry, Chinese Academy of Sciences, Changchun 130022, P. R. China; University of Science and Technology of China, Hefei 230026, P. R. China*

Xiaofei Tian − *State Key Laboratory of Polymer Physics and Chemistry, Changchun Institute of Applied Chemistry, Chinese Academy of Sciences, Changchun 130022, P. R. China; University of Science and Technology of China, Hefei 230026, P. R. China*

Xiaolei Xu − *State Key Laboratory of Polymer Physics and Chemistry, Changchun Institute of Applied Chemistry, Chinese Academy of Sciences, Changchun 130022, P. R. China;* orcid.org/0000-0002-4193-1819

Complete contact information is available at:
https://pubs.acs.org/10.1021/acs.macromol.2c01877

Notes

The authors declare no competing financial interest.

■ ACKNOWLEDGMENTS

W.-S.X. acknowledges the support from the National Natural Science Foundation of China (Nos. 22222307 and 21973089). J.C. acknowledges the support from the National Key Research and Development Program of China (No. 2018YFB1502302) and the National Natural Science Foundation of China (Nos. 22273013). This research used resources of the Network and Computing Center at Changchun Institute of Applied Chemistry, Chinese Academy of Sciences.

■ REFERENCES

(1) Purohit, P. K.; Inamdar, M. M.; Grayson, P. D.; Squires, T. M.; Kondev, J.; Phillips, R. Forces during bacteriophage DNA packaging and ejection. *Biophys. J.* **2005**, *88*, 851−866.

(2) Molineux, I. J.; Panja, D. Popping the cork: mechanisms of phage genome ejection. *Nat. Rev. Microbiol.* **2013**, *11*, 194−204.

(3) Hanhijärvi, K.; Ziedaite, G.; Pietilä, M. K.; Hæggström, E.; Bamford, D. DNA ejection from an archaeal virus—a single-molecule approach. *Biophys. J.* **2013**, *104*, 2264−2272.

(4) Rasmussen, C. J.; Vishnyakov, A.; Neimark, A. V. Translocation dynamics of freely jointed Lennard-Jones chains into adsorbing pores. *J. Chem. Phys.* **2012**, *137*, 144903.

(5) Luan, B.; Stolovitzky, G.; Martyna, G. Slowing and controlling the translocation of DNA in a solid-state nanopore. *Nanoscale* **2012**, *4*, 1068−1077.

(6) Dorfman, K. D. DNA electrophoresis in microfabricated devices. *Rev. Mod. Phys.* **2010**, *82*, 2903.

(7) Dorfman, K. D. The fluid mechanics of genome mapping. *AIChE J.* **2013**, *59*, 346.

(8) Glasgow, J.; Tullman-Ercek, D. Production and applications of engineered viral capsids. *Appl. Microbiol. Biotechnol.* **2014**, *98*, 5847−5858.

(9) Han, J.; Craighead, H. G. Separation of long DNA molecules in a microfabricated entropic trap array. *Science* **2000**, *288*, 1026−1029.

(10) Magill, M.; Waller, E.; de Haan, H. W. A sequential nanopore-channel device for polymer separation. *J. Chem. Phys.* **2018**, *149*, 174903.

(11) Wanunu, M.; Sutin, J.; McNally, B.; Chow, A.; Meller, A. DNA translocation governed by interactions with solid-state nanopores. *Biophys. J.* **2008**, *95*, 4716−4725.

(12) Branton, D.; Deamer, D. W.; Marziali, A.; Bayley, H.; Benner, S. A.; Butler, T.; Di Ventra, M.; Garaj, S.; Hibbs, A.; Huang, X.; et al. The potential and challenges of nanopore sequencing. *Nat. Biotechnol.* **2008**, *26*, 1146−1153.

(13) Atas, E.; Singer, A.; Meller, A. DNA sequencing and bar-coding using solid-state nanopores. *Electrophoresis* **2012**, *33*, 3437−3447.

(14) Postma, H. W. C. Rapid sequencing of individual DNA molecules in graphene nanogaps. *Nano Lett.* **2010**, *10*, 420−425.

(15) Marie, R.; Pedersen, J. N.; Bauer, D. L.; Rasmussen, K. H.; Yusuf, M.; Volpi, E.; Flyvbjerg, H.; Kristensen, A.; Mir, K. U. Integrated view of genome structure and sequence of a single DNA molecule in a nanofluidic device. *Proc. Natl. Acad. Sci. U. S. A.* **2013**, *110*, 4893−4898.

(16) Muthukumar, M. Mechanism of DNA transport through pores. *Annu. Rev. Biophys. Biomol. Struct.* **2007**, *36*, 435−450.

(17) Miné-Hattab, J.; Recamier, V.; Izeddin, I.; Rothstein, R.; Darzacq, X. Multi-scale tracking reveals scale-dependent chromatin dynamics after DNA damage. *Mol. Biol. Cell* **2017**, *28*, 3323−3332.

(18) Nagai, S.; Dubrana, K.; Tsai-Pflugfelder, M.; Davidson, M. B.; Roberts, T. M.; Brown, G. W.; Varela, E.; Hediger, F.; Gasser, S. M.; Krogan, N. J. Functional targeting of DNA damage to a nuclear pore-associated SUMO-dependent ubiquitin ligase. *Science* **2008**, *322*, 597−602.

(19) Zhou, D.-M.; Du, W.-F.; Xi, Q.; Ge, J.; Jiang, J.-H. Isothermal nucleic acid amplification strategy by cyclic enzymatic repairing for highly sensitive microRNA detection. *Anal. Chem.* **2014**, *86*, 6763−6767.

(20) Rousseau, B. J.; Shafei, S.; Migliore, A.; Stanley, R. J.; Beratan, D. N. Determinants of photolyase's DNA repair mechanism in mesophiles and extremophiles. *J. Am. Chem. Soc.* **2018**, *140*, 2853−2861.

(21) Groth, A.; Rocha, W.; Verreault, A.; Almouzni, G. Chromatin challenges during DNA replication and repair. *Cell* **2007**, *128*, 721−733.

(22) Bell, S.; Terentjev, E. M. Specific binding of a polymer chain to a sequence of surface receptors. *Sci. Rep.* **2017**, *7*, 1−8.

(23) Bell, S.; Terentjev, E. M. Kinetics of tethered ligands binding to a surface receptor. *Macromolecules* **2017**, *50*, 8810−8815.

(24) Muthukumar, M. Translocation of a confined polymer through a hole. *Phys. Rev. Lett.* **2001**, *86*, 3188.

(25) Muthukumar, M. Polymer escape through a nanopore. *J. Chem. Phys.* **2003**, *118*, 5174−5184.

(26) Panja, D.; Barkema, G. T.; Kolomeisky, A. B. Through the eye of the needle: recent advances in understanding biopolymer translocation. *J. Phys.: Condens. Matter* **2013**, *25*, 413101.

(27) Palyulin, V. V.; Ala-Nissila, T.; Metzler, R. Polymer translocation: the first two decades and the recent diversification. *Soft Matter* **2014**, *10*, 9016−9037.

(28) Sakaue, T. Dynamics of polymer translocation: A short review with an introduction of weakly-driven regime. *Polymers* **2016**, *8*, 424.

(29) Sarabadani, J.; Ala-Nissila, T. Theory of pore-driven and end-pulled polymer translocation dynamics through a nanopore: An overview. *J. Phys.: Condens. Matter* **2018**, *30*, 274002.

(30) Doi, M.; Edwards, S. F.*The Theory of Polymer Dynamics*; Oxford University Press: 1988.

(31) Cacciuto, A.; Luijten, E. Confinement-driven translocation of a flexible polymer. *Phys. Rev. Lett.* **2006**, *96*, 238104.

(32) Zhou, H.-X.; Zwanzig, R. A rate process with an entropy barrier. *J. Chem. Phys.* **1991**, *94*, 6147−6152.

(33) de Haan, H. W.; Sean, D.; Slater, G. W. Reducing the variance in the translocation times by prestretching the polymer. *Phys. Rev. E* **2018**, *98*, 022501.

(34) Magill, M.; Falconer, C.; Waller, E.; de Haan, H. W. Translocation time through a nanopore with an internal cavity is minimal for polymers of intermediate length. *Phys. Rev. Lett.* **2016**, *117*, 247802.

(35) Sean, D.; de Haan, H. W.; Slater, G. W. Translocation of a polymer through a nanopore starting from a confining nanotube. *Electrophoresis* **2015**, *36*, 682−691.

(36) Guérin, T.; Bénichou, O.; Voituriez, R. Non-Markovian polymer reaction kinetics. *Nat. Chem.* **2012**, *4*, 568−573.

(37) Grebenkov, D. S.; Oshanin, G. Diffusive escape through a narrow opening: new insights into a classic problem. *Phys. Chem. Chem. Phys.* **2017**, *19*, 2723−2739.

(38) Rubinstein, M.; Colby, R. H.*Polymer Physics*; Oxford University Press: 2003.

(39) Bickel, T. A note on confined diffusion. *Physica A* **2007**, *377*, 24−32.

(40) Weber, S. C.; Theriot, J. A.; Spakowitz, A. J. Subdiffusive motion of a polymer composed of subdiffusive monomers. *Phys. Rev. E* **2010**, *82*, 011913.

(41) Metzler, R.; Jeon, J.-H.; Cherstvy, A. G.; Barkai, E. Anomalous diffusion models and their properties: non-stationarity, non-

ergodicity, and ageing at the centenary of single particle tracking. *Phys. Chem. Chem. Phys.* **2014**, *16*, 24128−24164.

(42) Ma, Z.; Dorfman, K. D. Diffusion of knots along DNA confined in nanochannels. *Macromolecules* **2020**, *53*, 6461−6468.

(43) Guérin, T.; Levernier, N.; Bénichou, O.; Voituriez, R. Mean first-passage times of non-Markovian random walkers in confinement. *Nature* **2016**, *534*, 356−359.

(44) Korabel, N.; Waigh, T. A.; Fedotov, S.; Allan, V. J. Non-Markovian intracellular transport with sub-diffusion and run-length dependent detachment rate. *PLoS One* **2018**, *13*, e0207436.

(45) Allemand, J.-F.; Cocco, S.; Douarche, N.; Lia, G. Loops in DNA: an overview of experimental and theoretical approaches. *Eur. Phys. J. E* **2006**, *19*, 293−302.

(46) Yu, W.; Luo, K. Loop formation and stability of self-avoiding polymer chains. *Sci. China: Chem.* **2015**, *58*, 689−693.

(47) Levernier, N.; Bénichou, O.; Voituriez, R.; Guérin, T. Kinetics of rare events for non-Markovian stationary processes and application to polymer dynamics. *Phys. Rev. Res.* **2020**, *2*, 012057.

(48) Jeppesen, C.; Wong, J. Y.; Kuhl, T. L.; Israelachvili, J. N.; Mullah, N.; Zalipsky, S.; Marques, C. M. Impact of polymer tether length on multiple ligand-receptor bond formation. *Science* **2001**, *293*, 465−468.

(49) Satija, R.; Makarov, D. E. Generalized Langevin equation as a model for barrier crossing dynamics in biomolecular folding. *J. Phys. Chem. B* **2019**, *123*, 802−810.

(50) Amitai, A.; Kantor, Y.; Kardar, M. First-passage distributions in a collective model of anomalous diffusion with tunable exponent. *Phys. Rev. E* **2010**, *81*, 011107.

(51) Amitai, A.; Amoruso, C.; Ziskind, A.; Holcman, D. Encounter dynamics of a small target by a polymer diffusing in a confined domain. *J. Chem. Phys.* **2012**, *137*, 244906.

(52) Kantor, Y.; Kardar, M. Anomalous diffusion with absorbing boundary. *Phys. Rev. E* **2007**, *76*, 061121.

(53) Levernier, N.; Bénichou, O.; Guérin, T.; Voituriez, R. Universal first-passage statistics in aging media. *Phys. Rev. E* **2018**, *98*, 022125.

(54) Grigoriev, I. V.; Makhnovskii, Y. A.; Berezhkovskii, A. M.; Zitserman, V. Y. Kinetics of escape through a small hole. *J. Chem. Phys.* **2002**, *116*, 9574−9577.

(55) Vojta, T.; Halladay, S.; Skinner, S.; Janušonis, S.; Guggenberger, T.; Metzler, R. Reflected fractional Brownian motion in one and higher dimensions. *Phys. Rev. E* **2020**, *102*, 032108.

(56) Schuss, Z.; Singer, A.; Holcman, D. The narrow escape problem for diffusion in cellular microdomains. *Proc. Natl. Acad. Sci. U. S. A.* **2007**, *104*, 16098−16103.

(57) Singer, A.; Schuss, Z.; Holcman, D.; Eisenberg, R. S. Narrow escape, part I. *J. Stat. Phys.* **2006**, *122*, 437−463.

(58) Suma, A.; Micheletti, C. Pore translocation of knotted DNA rings. *Proc. Natl. Acad. Sci. U. S. A.* **2017**, *114*, E2991−E2997.

(59) Weber, S. C.; Spakowitz, A. J.; Theriot, J. A. Bacterial chromosomal loci move subdiffusively through a viscoelastic cytoplasm. *Phys. Rev. Lett.* **2010**, *104*, 238102.

(60) Schuss, Z. The narrow escape problem—a short review of recent results. *J. Sci. Comput.* **2012**, *53*, 194−210.

(61) Skaug, M. J.; Wang, L.; Ding, Y.; Schwartz, D. K. Hindered nanoparticle diffusion and void accessibility in a three-dimensional porous medium. *ACS Nano* **2015**, *9*, 2148−2156.

(62) Wu, H.; Wang, D.; Schwartz, D. K. Connecting hindered transport in porous media across length scales: From single-pore to macroscopic. *J. Phys. Chem. Lett.* **2020**, *11*, 8825−8831.

(63) Singer, A.; Schuss, Z.; Holcman, D. Narrow escape, Part II: The circular disk. *J. Stat. Phys.* **2006**, *122*, 465−489.

(64) Guérin, T.; Bénichou, O.; Voituriez, R. Reactive conformations and non-Markovian reaction kinetics of a Rouse polymer searching for a target in confinement. *Phys. Rev. E* **2013**, *87*, 032601.

(65) Grebenkov, D. S.; Metzler, R.; Oshanin, G. Full distribution of first exit times in the narrow escape problem. *New J. Phys.* **2019**, *21*, 122001.

(66) Zahedi, G.; Fazlali, A.; Hosseini, S.; Pazuki, G.; Sheikhattar, L. Prediction of asphaltene precipitation in crude oil. *J. Pet. Sci. Eng.* **2009**, *68*, 218−222.

(67) Adam, G.; Delbrück, M. In *Structural Chemistry and Molecular Biology*; Rich, A., Davidson, N., Eds.; Freeman: San Francisco, 1968; pp 198−215.

(68) Grebenkov, D. S.; Metzler, R.; Oshanin, G. Search efficiency in the Adam-Delbrück reduction-of-dimensionality scenario versus direct diffusive search. *New J. Phys.* **2022**, *24*, 083035.

(69) Hoseinpoor, S. M.; Nikoofard, N.; Ha, B.-Y. Characteristic time for the end monomers of a spherically confined polymer to find a nano-pore. *J. Chem. Phys.* **2021**, *154*, 114901.

(70) Shin, J.; Cherstvy, A. G.; Metzler, R. Kinetics of polymer looping with macromolecular crowding: effects of volume fraction and crowder size. *Soft Matter* **2015**, *11*, 472−488.

(71) Bian, Y.; Cao, X.; Li, P.; Zhao, N. Understanding chain looping kinetics in polymer solutions: crowding effects of microviscosity and collapse. *Soft Matter* **2018**, *14*, 8060−8072.